JACS
JOURNAL OF THE AMERICAN CHEMICAL SOCIETY
Article
pubs.acs.org/JACS

Synthesis and Properties of Endohedral Aza[60]fullerenes: $H_2O@C_{59}N$ and $H_2@C_{59}N$ as Their Dimers and Monomers

Yoshifumi Hashikawa,[†] Michihisa Murata,[†] Atsushi Wakamiya,[†] and Yasujiro Murata*[,†,‡]

[†]Institute for Chemical Research, Kyoto University, Uji, Kyoto 611-0011, Japan
[‡]JST, PRESTO, 4-1-8 Honcho, Kawaguchi, Saitama 332-0012, Japan

Supporting Information

ABSTRACT: The macroscopic-scale syntheses of the first endohedral aza[60]fullerenes $X@C_{59}N$ (X = H_2O, H_2) were achieved in two different ways: (1) synthesis from endohedral fullerene $H_2O@C_{60}$ as a starting material and (2) molecular surgical synthesis from a $C_{59}N$ precursor having a considerably small opening. In the neutral state of $H_2O@C_{59}N$, we expected the H-bonding interaction or repulsive N−O interaction between entrapped H_2O and a nitrogen atom on the $C_{59}N$ cage. However, an attractive electrostatic N−O interaction was suggested from the results of variable temperature NMR, nuclear magnetic relaxation times (T_1, T_2), and density functional theory (DFT) calculations. Upon the reaction with acetone via cationic intermediate $C_{59}N^+$, we found a difference in reaction rates between $H_2O@C_{59}N$ and $H_2@C_{59}N$ dimers (observed reaction rates: $k'(H_2O)/k'(H_2)$ = 1.74 ± 0.16). The DFT calculations showed thermal stabilization of $C_{59}N^+$ by entrapped H_2O through the electrostatic interaction.

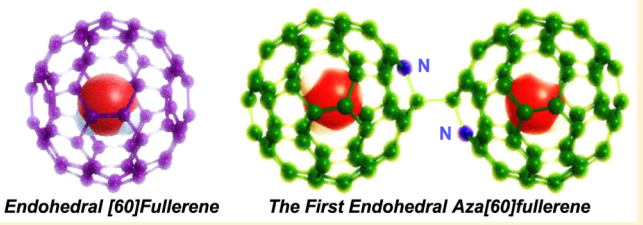

INTRODUCTION

Fullerene C_{60} has an internal space with a diameter of ca. 3.7 Å, which is suitable for accommodating a small atom or molecule. Several endohedral fullerenes $X@C_{60}$ (X = atom(s) and molecule(s)) have been synthesized in macroscopic quantities. Examples of an entrapped molecule include not only neutral species such as He,[1] Ne,[1] H_2,[2] and H_2O[3] but also radical or cationic species such as N,[4] P,[5] or Li^+.[6] Recently, the nature of an H_2O molecule inside the C_{60} cage has been investigated. In 2012, Levitt and co-workers observed an apparent *ortho*−*para* conversion of entrapped H_2O as well as a rapid isotropic rotation inside the restricted space at temperatures below 20 K.[7] In 2014, Aoyagi et al. reported an increase of the dielectric permittivity for a single crystal of $H_2O@C_{60}$ upon cooling to 8 K.[8]

In contrast, reports on synthetic development of a heterofullerene family are quite limited. In the 1990s, heterofullerenes $C_{59}Y$ (Y = B,[9] N,[10] Si,[11] Ir,[12] and Pt[12]) had been reported, and their existence was confirmed only under mass conditions in gas-phase without any structural information except for computational predictions. Despite some substantial evidence for metallic endohedral heterofullerenes (vide infra), examples of effective syntheses are confined almost exclusively to azafullerenes $C_{n-1}N$ (n = 60, 70). In 1995, Wudl and co-workers reported the first open-cage C_{60} derivative which has a ketolactam moiety on the opening.[13] In the same year, they achieved the synthesis of bis(aza[60]fullerenyl) $(C_{59}N)_2$ from the open-cage C_{60} derivative.[14] They proposed that a MEM-substituted ketolactam moiety is a key structure to form a $C_{59}N$ skeleton.[15] In the next year, Hirsch and Nuber succeeded in the synthesis of $(C_{59}N)_2$ by another method and also reported bis(aza[70]fullerenyl) $(C_{69}N)_2$.[16] These discoveries provide useful methods for synthesizing N-doped fullerenes in bulk quantities.

In recent years, combination of *endohedral fullerenes* and *heterofullerenes* has been attracting great attention. To date, these two types of chemical modifications have been almost independently developed. The first evidence of endohedral heterofullerenes was reported by Smalley and co-workers in 1991.[17] They revealed that the Fourier transform ion cyclotron resonance (FT-ICR) mass spectrum of a material prepared from a boron/graphite composite rod showed an existence of $K@C_{59}B$ and $K@C_{58}B_2$ which were accidentally formed by contamination of KCl. In 1999, Akasaka and co-workers reported the synthesis of $La@C_{82}(NCH_2Ph)$ by an addition reaction of benzyl azide to $La@C_{82}$ and found that the fast atom bombardment (FAB) mass spectrum of $La@C_{82}(NCH_2Ph)$ exhibited a fragment peak corresponding to endohedral heterofullerene $La@C_{81}N^+$.[18] They also proved the existence of $La_2@C_{79}N^+$ from the FAB mass fragmentations of $La_2@C_{80}(NCH_2Ph)$. In 2008, Balch, Dorn, and co-workers reported the preparation and isolation of dimetallic endohedral aza[80]fullerenes $M_2@C_{79}N$ (M = Y, Tb).[19] They prepared $M_2@C_{79}N$ from cored graphite rods packed with Y_2O_3 or Tb_4O_7 by applying the Krätschmer−Huffman electric-arc method. The crystallographic data of $Tb_2@C_{79}N$ cocrystallized with NiOEP (OEP, octaethylporphyrin) conclusively excluded alternative possibilities of chemical formula such as $Tb_2CN@C_{78}$ and $Tb_2C_2@C_{77}N$. The crystallographic analysis of $Tb_2@$

Received: December 7, 2015
Published: March 18, 2016

DOI: 10.1021/jacs.5b12795
J. Am. Chem. Soc. 2016, 138, 4096−4104

Scheme 1. Synthesis of Endohedral Bis(aza[60]fullerenyl) Encapsulating Water Molecule(s)

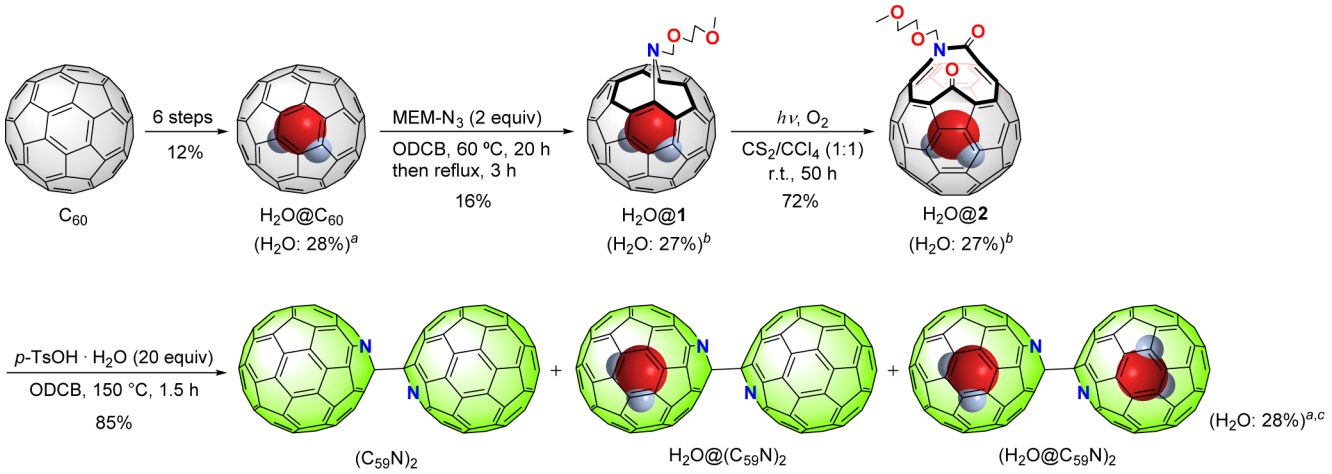

[a]Encapsulation ratio estimated by APCI mass. [b]Estimated by ^{1}H NMR. [c]Apparent value for a mixture of dimers of $C_{59}N$ and $H_2O@C_{59}N$.

Scheme 2. Synthesis of Endohedral Bis(aza[60]fullerenyl) Encapsulating Hydrogen Molecule(s)

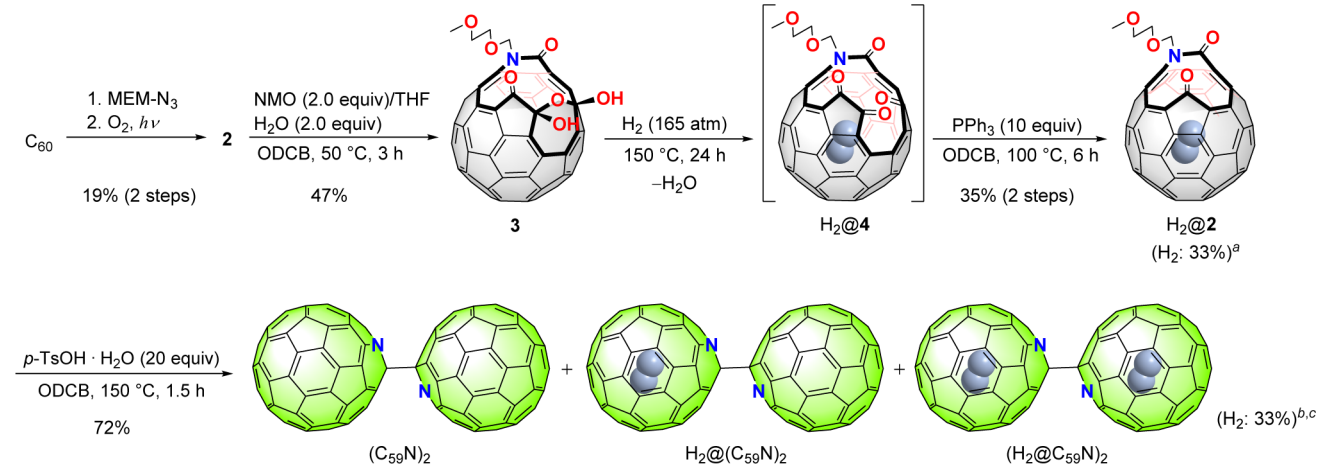

[a]Encapsulation ratio estimated by ^{1}H NMR. [b]Estimated by APCI mass. [c]Apparent value for a mixture of dimers of $C_{59}N$ and $H_2@C_{59}N$.

$C_{79}N$ showed that there is no specific interaction between a nitrogen atom on the cage and a nickel atom of the NiOEP molecule which was located outside the cage. In the same manner, $Gd_2@C_{79}N$ was synthesized by the group in 2011 from graphite powder containing Gd_2O_3 with metallic Cu as a catalyst and isolated in ~0.05−0.1% as a relative yield ratio of $Gd_2@C_{79}N/C_{60}$.[20] In addition, Stevenson, Zhang, and co-workers presented experimental evidence of trimetallic nitride endohedral aza[80]fullerene, $La_3N@C_{79}N$ in 2009.[21] They applied the chemically adjusting plasma temperature, energy, and reactivity (CAPTEAR)[22] approach to a graphite rod packed with Sc_2O_3/La_2O_3. The matrix assisted laser desorption ionization (MALDI) mass spectrum of the resulting soot extract contained molecular ion peaks of C_{60}, C_{70}, $Sc_3N@C_{80}$, and $LaSc_2N@C_{80}$ as major components together with $La_3N@C_{79}N$ as a minor component in spite of the absence of $La_3N@C_{80}$.

Of importance is to study properties and behaviors of a small molecule inside the cage of N-doped fullerene. Doping of a nitrogen atom on the carbon cage is expected to influence the nature of the inside of the cage. Thus, we focused on the rational preparation of endohedral heterofullerenes using the $C_{59}N$ cage. We studied two possible routes to obtain sufficient amount of endohedral aza[60]fullerene $X@C_{59}N$: (1) synthesis from endohedral fullerene $X@C_{60}$ and (2) molecular surgical synthesis[23] which contains a size-expansion of an opening of $C_{59}N$ precursor **2**, insertion of a guest molecule, and closing of the opening. Here we report these two synthetic pathways, characteristic NMR properties, and difference in reactivity between $H_2O@C_{59}N$ and $H_2@C_{59}N$.

RESULTS AND DISCUSSION

Synthesis of $H_2O@C_{59}N$ Dimers. In a way analogous to the preparation of $(C_{59}N)_2$,[14] we obtained the first endohedral aza[60]fullerene from $H_2O@C_{60}$. The synthetic pathway was shown in Scheme 1. According to the reported procedures,[3,24] $H_2O@C_{60}$ was synthesized from C_{60} in 12% overall yield (6 steps). First, the 1,3-dipolar cycloaddition reaction of 2-methoxyethoxymethyl azide (MEM-N_3)[13,25] was conducted using $H_2O@C_{60}$ with the encapsulation ratio of 28%. After chromatographic purification, $H_2O@$**1** was obtained in 16% yield. Subsequently, we synthesized $H_2O@$**2** by photooxygenation[13] of $H_2O@$**1** under O_2 atmosphere. The encapsulation ratio of $H_2O@$**2** was determined to be 27% by ^{1}H NMR spectrum. By applying the Wudl's conditions,[14] we obtained $H_2O@C_{59}N$ as its dimers in 85% yield (Scheme 1). The overall

DOI: 10.1021/jacs.5b12795
J. Am. Chem. Soc. 2016, 138, 4096−4104

yield is calculated to be 1.2% from C_{60}. We also synthesized pure $(H_2O@C_{59}N)_2$ from $H_2O@C_{60}$ with the encapsulation ratio of 100%.

Synthesis of $H_2@C_{59}N$ Dimers. Open-cage fullerene derivatives have great potential as precursors not only for endohedral fullerenes but also for heterofullerenes. As described in the literature,[26] the way to introduce a hydrogen molecule into the cage of a ketolactam derivative of C_{60} (**2**) has already developed. As shown in Scheme 2, an 11-membered-ring opening of **2** was first enlarged by the reaction with *N*-methylmorpholine *N*-oxide (NMO) to form a 12-membered-ring opening (**3**). Further enlargement was achieved by heating, which led to in-situ generation of a 15-membered-ring opening (**4**), and subsequently H_2-insertion was performed. Under the optimized conditions (150 °C, 165 atm, 24 h) (Table S1), the encapsulation ratio of H_2 reached to 33%, which was confirmed by ^{1}H NMR spectrum. The opening of $H_2@$**4** was partially closed to afford $H_2@$**2** while retaining the ratio of entrapped H_2. Thus, obtained $H_2@$**2** can be considered as a possible precursor of endohedral aza[60]fullerene $H_2@C_{59}N$.[26] In a similar way, we attempted H_2O-insertion using **3** as a host molecule (150 °C, 10 000 atm, 24 h in PhCl), but no encapsulation was observed by atmospheric pressure chemical ionization (APCI) mass and ^{1}H NMR spectra. This suggests that the 15-membered-ring opening of **4** is still small for H_2O to be inserted into the cage. Finally, we obtained $H_2@C_{59}N$ as its dimers by the reaction of $H_2@$**2** (H_2: 33%) under the Wudl's conditions[14] in 72% yield (Scheme 2). The overall yield was 2.2% from C_{60}, which is two times higher than that of $H_2O@C_{59}N$ dimers synthesized by the method described above. We think the latter synthetic approach is more effective to gain endohedral aza[60]fullerene $X@C_{59}N$, especially for encapsulating a molecule such as H_2 or He, which are smaller than H_2O.

Characterization by Mass Spectroscopy and HPLC Analysis. The APCI mass spectrum in positive ion mode of $H_2O@C_{59}N$ dimers showed two signals corresponding to monomeric $C_{59}N^+$ (*m*/*z* 722.0011) and $H_2O@C_{59}N^+$ (*m*/*z* 740.0161) generated by cleavage of the C(sp^3)−C(sp^3) bond connecting two $C_{59}N$ cages, instead of signals of dimers (Figure 1a). Assuming the similar ionization abilities both of $C_{59}N$ and $H_2@C_{59}N$, an apparent encapsulation ratio of $H_2O@C_{59}N$ dimers was determined to be 28% from the mass intensities. This indicates no escape of entrapped H_2O in the course of the reactions. The fragment ion peaks of $H_2@C_{59}N$ dimers were observed in negative ion mode at *m*/*z* 722.0065 and 724.0166, respectively, corresponding to monomeric $C_{59}N^-$ and $H_2@C_{59}N^-$ with no signal of dimers (Figure 1b). An apparent encapsulation ratio of $H_2@C_{59}N$ dimers was estimated to be 33% from the mass intensities.

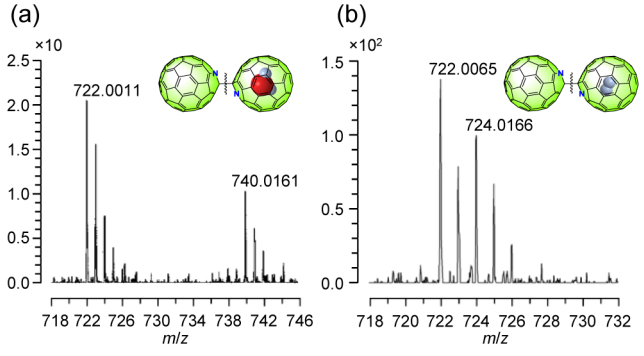

Figure 1. APCI mass spectra of (a) $H_2O@C_{59}N$ dimers in positive ion mode and (b) $H_2@C_{59}N$ dimers in negative ion mode.

The high-performance liquid chromatography (HPLC; Buckyprep column, toluene, 50 °C) analysis clearly showed the dimeric configuration of $X@C_{59}N$ in an analogous way for empty $C_{59}N$ (retention time t_R, 7.10 min for $HC_{59}N$ and 14.0 min for $(C_{59}N)_2$). It was also found that $H_2O@C_{59}N$ dimers comprise three components (Figure 2a), corresponding to

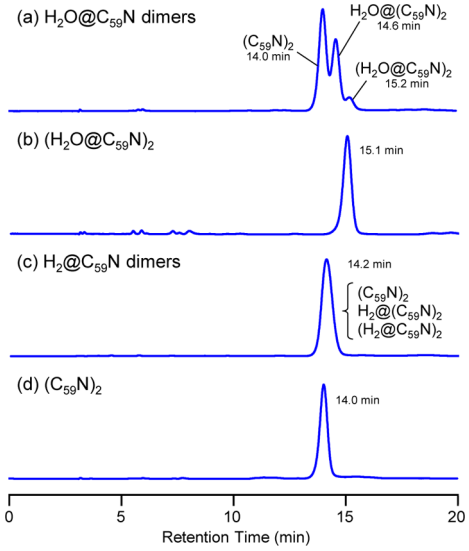

Figure 2. HPLC (Buckyprep column, toluene, 50 °C) charts of (a) $H_2O@C_{59}N$ dimers, (b) pure $(H_2O@C_{59}N)_2$, (c) $H_2@C_{59}N$ dimers, and (d) $(C_{59}N)_2$.

empty $(C_{59}N)_2$ (t_R = 14.0 min), singly encapsulating $H_2O@(C_{59}N)_2$ (t_R = 14.6 min), and doubly encapsulating $(H_2O@C_{59}N)_2$ (t_R = 15.2 min). These results were quite similar to those observed for $H_2O@C_{60}$ dimers.[27] The composition ratio of $(C_{59}N)_2$, $H_2O@(C_{59}N)_2$, and $(H_2O@C_{59}N)_2$ was determined to be 55:39:6 according to the peak area ratio, which is in close accordance with the value (53:40:7) predicted from the encapsulation ratio of precursor $H_2O@$**2** (H_2O: 27%). In a similar fashion of $H_2O@C_{59}N$ dimers, $H_2@C_{59}N$ dimers should contain $(C_{59}N)_2$, $H_2@(C_{59}N)_2$, and $(H_2@C_{59}N)_2$ with the production ratio of 45:44:11. However, only one peak was observed at the retention time of 14.2 min, which is almost the same value of the empty one (t_R = 14.0 min) but slightly broadened compared to the empty one (Figure 2c,d). These results indicate that there is a stronger interaction between $H_2O@C_{59}N$ dimers and a stationary phase (silica-based column modified with *pyrene*) compared to $H_2@C_{59}N$ dimers, probably due to the difference in van der Waals interaction between the $C_{59}N$ cage and entrapped molecules.

Chemical Shifts. The ^{1}H NMR signals of H_2O and H_2 inside the $C_{59}N$ cage were shown in Figure 3, as well as residual H_2O and free H_2 in ODCB-d_4 at room temperature. The proton signals of $X@C_{59}N$ dimers containing $(X@C_{59}N)_2$ and $X@(C_{59}N)_2$ were fully overlapped as a sharp singlet at δ −6.96 ppm for entrapped H_2O and δ −3.43 ppm for entrapped H_2, respectively (Figure 3a,b). This shows that there is no detectable magnetic interaction between two entrapped molecules which were separated by the $C_{59}N$ cage.[27] In comparison with residual H_2O (δ 1.37 ppm) and free H_2 (δ 4.54 ppm) in ODCB-d_4 (Figure 3c), an entrapped molecule

DOI: 10.1021/jacs.5b12795
J. Am. Chem. Soc. 2016, 138, 4096−4104

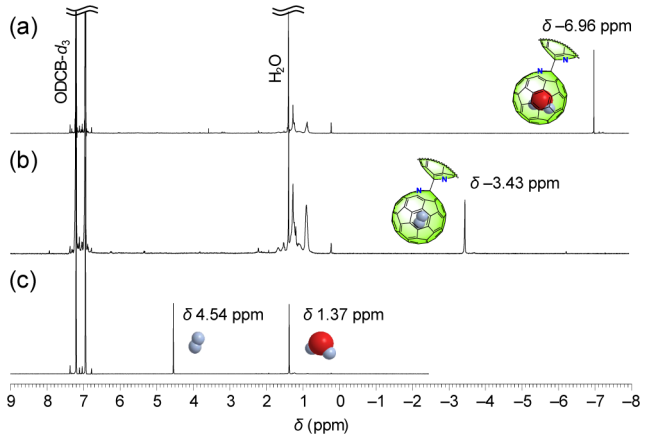

Figure 3. ^{1}H NMR spectra (500 MHz, ODCB-d_4, r.t.) of (a) H_2O@$C_{59}N$ dimers with a 55:39:6 ratio of $(C_{59}N)_2$, H_2O@$(C_{59}N)_2$, and $(H_2O@C_{59}N)_2$; (b) H_2@$C_{59}N$ dimers with a 45:44:11 ratio of $(C_{59}N)_2$, H_2@$(C_{59}N)_2$, and $(H_2@C_{59}N)_2$; and (c) a 3:4 mixture of free H_2 and H_2O.

inside the $C_{59}N$ cage displayed a significant upfield-shift by ca. −8 ppm, reflecting slightly larger shielding effects than C_{60} (ca. −6 ppm).[2,3] The theoretical calculations[28] of NICS(0) for each hexagon and pentagon were conducted for C_{60}, $(C_{59}N)_2$, and $MeC_{59}N$ at the HF/6-311G(d,p)//B3LYP/6-31G(d) level of theory. The results suggested a decrease in antiaromaticity of all five-membered rings of $C_{59}N$, especially in an N-containing five-membered ring: NICS(0) + 8.17 for C_{60}, −2.26 to +6.97 for $(C_{59}N)_2$, and −3.28 to +6.82 for $MeC_{59}N$ (Figures S24–S26).

Variable Temperature NMR Experiments. The temperature dependence of chemical shifts is primarily associated with the electronic structures surrounding the nuclei or the degree of inter- and intramolecular interactions.[29] The variable temperature (VT) NMR measurements were performed at the temperature range of 260−360 K in ODCB-d_4. The upper limit was set to 360 K to avoid the formation of $C_{59}N$ radicals, and the lower limit was set to 260 K in consideration of the low solubility of dimeric $C_{59}N$ as well as the melting point of ODCB-d_4. The results showed that the temperature dependence of chemical shifts for entrapped H_2O is slightly stronger than that for entrapped H_2 (0.76 ppb/K for H_2@C_{60}, 0.75 ppb/K for H_2@$C_{59}N$ dimers, 0.91 ppb/K for H_2O@C_{60}, and 1.35 ppb/K for H_2O@$C_{59}N$ dimers) (Figure 4a, Figure S27, and

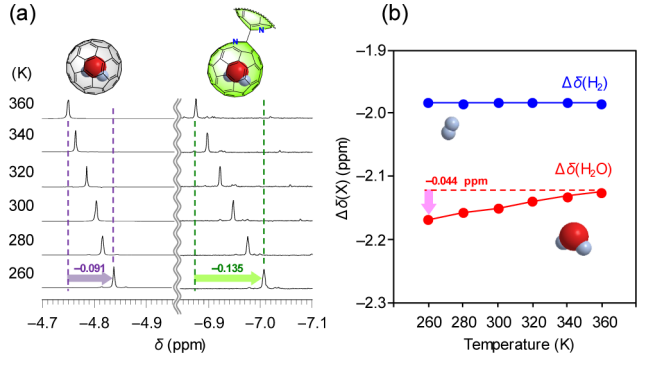

Figure 4. (a) ^{1}H NMR spectra (500 MHz, ODCB-d_4, 260−360 K) of H_2O@C_{60} and H_2O@$C_{59}N$ dimers and (b) chemical shifts of X@$C_{59}N$ dimers with reference to X@C_{60}, $\Delta\delta(X) = \delta(X@C_{59}N\ \text{dimers}) - \delta(X@C_{60})$.

Table S6). These chemical shift profiles most likely arise from the size effect of entrapped molecules (H_2O molecule is somewhat larger than H_2 molecule and might be in closer contact to the wall of the carbon cage.[30a]). However, the remarkably larger shift for H_2O@$C_{59}N$ dimers seems to be affected by an additional factor. To discuss in more detail, the difference in chemical shifts $\Delta\delta(X)$ was defined as the following equation and plotted as a function of temperature (Figure 4b).

$$\Delta\delta(X) = \delta(X@C_{59}N\ \text{dimers}) - \delta(X@C_{60})$$

In contrast to the $|\Delta\delta(H_2)|$ values without temperature dependence, the $|\Delta\delta(H_2O)|$ values became larger with decreasing temperatures, indicating the stronger shielding effects for H_2O in $C_{59}N$ (Figure 4b). This suggests the existence of a certain kind of intramolecular interactions which are dominant at lower temperatures and may restrict the rotational motion of entrapped H_2O. We first considered the possibility of hydrogen bonding effect between entrapped H_2O and nitrogen atom on the $C_{59}N$ cage. Generally, hydrogen bonding results in downfield shift due to electron-deficient protons of H_2O (deshielding effect). However, the chemical shift of H_2O@$C_{59}N$ dimers monotonically moved to upfield with decreasing temperatures. A plausible explanation for this phenomenon is that the rotational motion of H_2O in $C_{59}N$ is more restricted than that for H_2O@C_{60} by weak intramolecular interaction different from hydrogen bonding effect. This might account for the temperature dependence of chemical shifts for H_2O@$C_{59}N$ dimers. We cannot clearly demonstrate this hypothesis from only the results of the VT NMR experiments.

Relaxation Times. We found that the full widths at half-maximum of the proton signals of entrapped H_2 were approximately 2.5 times larger than that of entrapped H_2O, regardless of the type of fullerene cages such as C_{60} and $C_{59}N$. In general, the line width of the NMR signal is inversely proportional to the relaxation time required for nucleic spins excited by a radio frequency pulse to return to thermal equilibrium. In this case, the relaxation time of entrapped H_2 inside the fullerene cage is known to be shorter than that of entrapped H_2O under the influence of the dipole−dipole interaction depending on a short distance between two protons.[31] The mechanism of nuclear magnetic relaxation is commonly related to molecular motions. To gain further insights into the dynamics of entrapped molecules, we focused on the proton magnetic relaxation time for X@$C_{59}N$ dimers and X@C_{60}.

The spin−lattice relaxation times T_1 of entrapped H_2 and H_2O were measured by the inversion recovery method in ODCB-d_4 at 300 K at a field strength of 500 MHz (Figure 5a,c, Figures S28a,c and S29a,c, and Tables S7 and S8). The T_1 values of H_2@C_{60} and H_2O@C_{60} were determined to be 0.101 and 0.615 s, respectively, being in good agreement with the reported value in toluene-d_8 at 300 K.[30] In the case of entrapped H_2, there was almost no difference between the T_1 values of H_2@C_{60} (0.101 s) and H_2@$C_{59}N$ dimers (0.113 s), suggesting the similar molecular motion of the hydrogen molecule inside each cage. For entrapped H_2O, the T_1 value of H_2O@$C_{59}N$ dimers (1.72 s) is approximately three times longer than that for H_2O@C_{60} (0.615 s) (Figure 5c). The contributions to the longer T_1 values may include the influences of (1) rotation of entrapped H_2O, (2) N···H_2O interaction, (3) rotation of fullerene cage, and (4) residual $C_{59}N$ radical. Because of little difference of the T_1 values between H_2@C_{60} and H_2@$C_{59}N$ dimers, the latter contributions (3 and 4) could

DOI: 10.1021/jacs.5b12795
J. Am. Chem. Soc. 2016, 138, 4096−4104

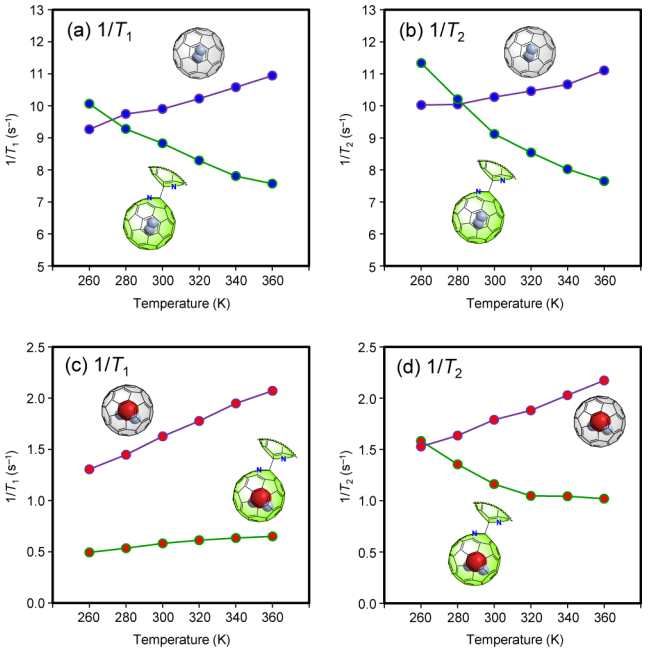

Figure 5. Relaxation rates (500 MHz, ODCB-d_4, 260−360 K), (a) $1/T_1$ for entrapped H_2, (b) $1/T_2$ for entrapped H_2, (c) $1/T_1$ for entrapped H_2O, and (d) $1/T_2$ for entrapped H_2O: blue points on a purple line, $H_2@C_{60}$; blue points on a green line, $H_2@C_{59}N$ dimers; red points on a purple line, $H_2O@C_{60}$; red points on a green line, $H_2O@C_{59}N$ dimers. The T_1 and T_2 values were measured by using inversion recovery method and the CPMG method, respectively. These values are the average of at least two measurements having errors within 5% and follow the general trend ($T_1 \geq T_2$) at each temperature.

be ruled out. However, the former contributions (1 and 2) still remain.

To unveil the detailed relaxation mechanism and the dynamic behavior of entrapped molecules, spin−lattice relaxation times T_1 were measured over the temperature range of 260−360 K in a 20 K interval, as well as spin−spin relaxation times T_2 by applying the CPMG (Carr−Purcell−Meiboom−Gill) method (Figure 5b,d, Figures S28b,d and 29b,d, and Tables S9 and S10). All of the T_2 values followed the general trend ($T_1 \geq T_2$). As mentioned in the literature,[30a] the T_1 values of $H_2@C_{60}$ in toluene-d_8 vary depending on the spin relaxation at higher temperatures (>240 K). The spin−rotation interactions must be enhanced with increasing temperature and lead to rapid relaxation.[30a] The temperature dependence of the T_2 values of $H_2@C_{60}$ was in agreement with this explanation (Figure 5b). In contrast, the T_2 relaxation of $H_2@C_{59}N$ dimers became rapid at lower temperatures. The origin of the rapid relaxation at lower temperatures is considered to be a dipole−dipole interaction, which should be stronger with decreasing temperature according to the faster reorientation of the magnetic dipoles. Note that $H_2@C_{60}$ has maximum point $T_{1,max}$ in toluene-d_8 at 240 K, and the major relaxation mechanism is a dipole−dipole interaction at temperatures below $T_{1,max}$ while a spin−rotation interaction becomes predominant at temperatures above $T_{1,max}$.[30a] For $H_2@C_{59}N$ dimers, the wider temperature range of the dipole−dipole interaction was found to be a major relaxation mechanism, and the maximum point of T_1 was not observed within the measured range. The possible reason is an additional dipolar interaction between nuclei ^1H (I = 1/2) of H_2 and ^{14}N (I = 1)/^{15}N (I = 1/2) in $C_{59}N$. On the other hand, for $H_2O@C_{60}$, the temperature dependence of T_1 and T_2 values exhibited a typical spin−rotation mechanism in an analogous way for $H_2@C_{60}$. However, $H_2O@C_{59}N$ dimers have three-times longer T_1 values compared to $H_2O@C_{60}$, probably due to the restrained rotational molecular motion (Figure 5c). Though the major relaxation mechanism for $H_2O@C_{59}N$ dimers seems to be the spin−rotation interaction, such interaction cannot be explained from the T_2 values because its temperature dependence was totally different from that for $H_2O@C_{60}$ whose magnetic relaxation mainly relies on the spin−rotation interaction (Figure 5d). According to the computational results of the electrostatic potentials for model compound $HC_{59}N$ (MP2/6-31G(d,p)//M06-2X/6-31G(d,p)) (Figure 6a), unexpectedly,

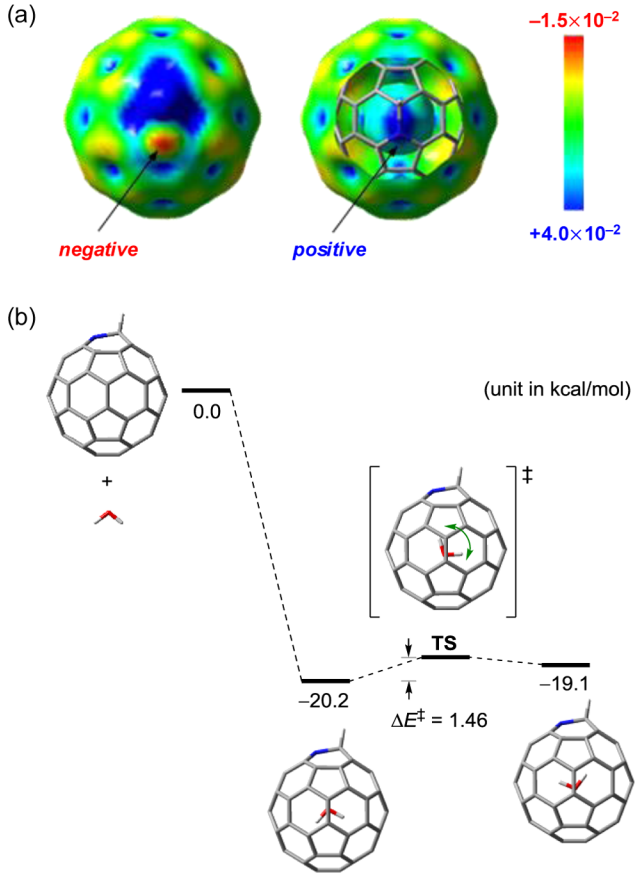

Figure 6. DFT calculations: (a) electrostatic potentials of $H_2O@HC_{59}N$ (MP2/6-31G(d,p)//M06-2X/6-31G(d,p)) and (b) relative energies for two conformers of $H_2O@HC_{59}N$ and TS (M06-2X/6-31G(d,p)).

the positive charge was distributed on the nitrogen atom on the inner surface of the $HC_{59}N$ cage, whereas the nitrogen atom was negatively charged on the outer surface. Additionally, we found two conformers of $H_2O@HC_{59}N$ having different molecular orientations of H_2O at the M06-2X/6-31G(d,p) level of theory (Figure 6b). The most stable conformer adopts a structure where the positive potential located on the backside of the nitrogen atom should be canceled out by the negative charge of lone pair electrons of the oxygen atom in entrapped H_2O. The rotational barrier of entrapped H_2O inside the $HC_{59}N$ cage was also determined to be 1.46 kcal/mol. These results suggest the electrostatic interaction between entrapped H_2O and the nitrogen atom. For the above reasons, the

DOI: 10.1021/jacs.5b12795
J. Am. Chem. Soc. 2016, 138, 4096−4104

plausible relaxation mechanism for $H_2O@C_{59}N$ dimers is considered as follows: the rotational motion restricted by the N−O interaction would reduce the effect of the spin−rotation interaction, and the magnetic energy coherently induced on the nuclei should move to the $C_{59}N$ cage via electrostatic N−O interaction; then, further energy transfer would occur from the cage to the lattice.

Here, we discuss again the DFT calculations which suggest the positively charged nitrogen atom on the inner surface of $HC_{59}N$. We calculated electrostatic potentials for additional related compounds: the simplest amine (DABCO) and amine embedded into the curved π-conjugated system (diazabuckybowl and pentabenzoazacoranulene[32]) (Figure S31). According to the calculations, DABCO has negatively charged nitrogen atom on the outer surface due to naked lone pair electrons. The positive potential was also found inside the caged structure of DABCO. Diazabuckybowl exhibited a similar potential map despite reduced sp^3-amine character, which was induced by the curved π-conjugation. In the case of pentabenzoazacoranulene, the positive charge was suggested to be distributed on the backside of the nitrogen atom in an analogous way for $HC_{59}N$ even though negative potential was not found on the outer surface based on the sp^2-pyrrol character. In all examples above, however, it would be difficult to discriminate this kind of bilateral potential character experimentally. As mentioned above, we were able to provide elusive evidence of the positive potential of the backside of the nitrogen atom using the unique molecular system $H_2O@RC_{59}N$.

Reactivity. For elucidation of the difference in reactivity between $H_2O@C_{59}N$ and $H_2@C_{59}N$ dimers, we made a choice of the known reaction of $(C_{59}N)_2$ with acetone under oxidative conditions.[33] The reaction mechanism was explained as follows: thermal dissociation of $(C_{59}N)_2$ to give two $C_{59}N$ radicals, oxidation of $C_{59}N$ radicals to $C_{59}N^+$ by O_2, and electrophilic attack to enolizable ketones to afford Mannich bases involving a $C_{59}N$ sphere ($CH_3COCH_2C_{59}N$, **5**). If there is an undisputed interaction between polar H_2O and cationic center of $C_{59}N^+$, the difference in reactivity based on the stabilization of $C_{59}N^+$ by entrapped H_2O would be expected. Recently, regarding an enantiospecific *cis*−*trans* isomerization of chiral fulleropyrrolidines, Martín and co-workers reported that anionic intermediate $H_2O@RC_{60}^-$ should be stabilized by the intramolecular hydrogen bonding induced by entrapped H_2O inside the C_{60} cage.[34]

First, we conducted the reaction using $H_2O@C_{59}N$ and $H_2@C_{59}N$ dimers separately (Scheme 3). The reaction progress was monitored by HPLC, and it was almost completed within 20 min at 150 °C. After chromatographic purification, X@**5** was obtained in similar yields for both H_2O and H_2. The proton signals of X@**5** in ODCB-d_4 appeared at δ −7.34 ppm for H_2O and −3.87 ppm for H_2, which were distinguishable from parent $X@C_{59}N$ dimers.

For the competition experiment, we subsequently prepared a mixture of $X@C_{59}N$ dimers with a 1:1 encapsulation ratio of H_2O and H_2 ($H_2O@C_{59}N/H_2@C_{59}N/C_{59}N$ = 22/22/56). The encapsulation ratio was determined by ^{1}H NMR spectrum (Figure 7b, **A**). The reaction was conducted at 100 °C in ODCB-d_4, and the reaction progress was monitored by ^{1}H NMR. The results are shown in Figure 7. After 0.5 h (point **B**), the molar ratio of starting material to target compound is ca. 2:1 for $H_2@C_{59}N$ dimers and ca. 1:2 for $H_2O@C_{59}N$ dimers, indicating the faster reaction for $H_2O@C_{59}N$ dimers.

Scheme 3. Synthesis of 1-Azafullerenylpropan-2-one Encapsulating a Small Molecule, X@5 (X = H_2O, H_2)

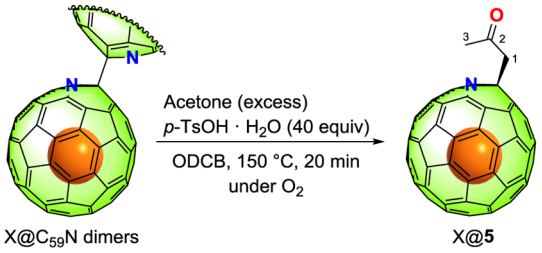

X	encapsulation ratio (%)		isolated yield (%)
	$X@C_{59}N$ dimers[a]	X@**5**[b]	
H_2O	26	26	67
H_2	29	30	63

[a]Estimated by APCI MS. [b]Estimated by ^{1}H NMR.

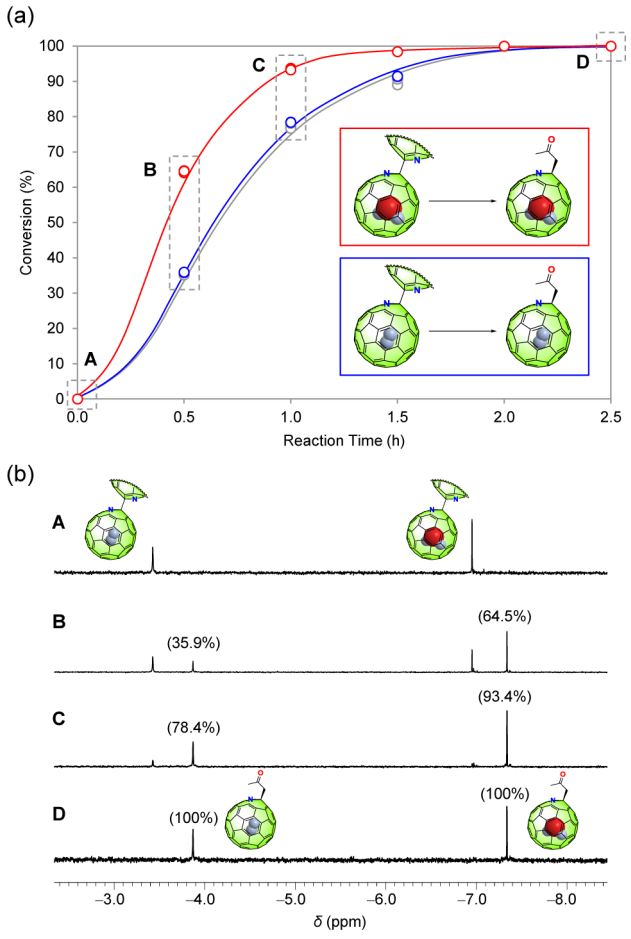

Figure 7. Competition experiment of $X@C_{59}N$ dimers (X = H_2O, H_2) with acetone at 100 °C in O_2 atmosphere under acidic conditions: (a) changes in conversion against reaction time and (b) selected ^{1}H NMR spectra (500 MHz, ODCB-d_4, r.t.) at each point of **A**−**D**. All values of conversion were determined by integrated ^{1}H NMR signals of three measurements. The four singlet signals correspond to $H_2@C_{59}N$ dimers (−3.43 ppm), $H_2@$**5** (−3.87 ppm), $H_2O@C_{59}N$ dimers (−6.96 ppm), and $H_2O@$**5** (−7.34 ppm), respectively.

The keto form of acetone is more stable than the enol form under acidic conditions. However, during the reaction, the enol form of acetone should be constantly formed in the keto−enol

DOI: 10.1021/jacs.5b12795
J. Am. Chem. Soc. 2016, 138, 4096−4104

tautomeric equilibrium while the enol form is consumed to afford Mannich base X@**5**. Therefore, if the concentration of enolizable acetone is high enough compared to X@$C_{59}N$ dimers and X@$C_{59}N^+$ is so reactive that the electrophilic addition to the enol form of acetone promptly takes place, this reaction can be assumed as pseudo-first-order reaction in both cases where X@$C_{59}N$ dimers are in pre-equilibrium with their radicals and where the changes in concentration of X@$C_{59}N$ radicals are much smaller than the formation rate of X@$C_{59}N^+$. Because the reaction rate should heavily depend on the step of $C_{59}N^+$ formation as demonstrated in the previous report,[33] we roughly estimated the apparent rate constants k' under the assumption of pseudo-first-order reaction expressed as follows:

$$-dC/dt = k'C \quad (C = [X@C_{59}N \text{ dimers}])$$

The concentrations of X@$C_{59}N$ dimers and X@$RC_{59}N$ were determined by the integration of proton signals for entrapped molecules. We obtained the concentration of empty adduct **5** by subtracting the concentration of X@$RC_{59}N$ from the concentration of acetone-adducts determined from integration of overlapped proton signals of α-H on C1 of oxopropyl group. (The labeling numbers are shown in Scheme 3.) Using these values, the concentration of empty $(C_{59}N)_2$ was also estimated. According to the rate law, we obtained the pseudo-first-order rate constant k' (10^4 s^{-1}) from the slope of plots as ln (C/C_0) versus reaction time (Figure 8): 7.50 ± 0.33 for $H_2O@C_{59}N$

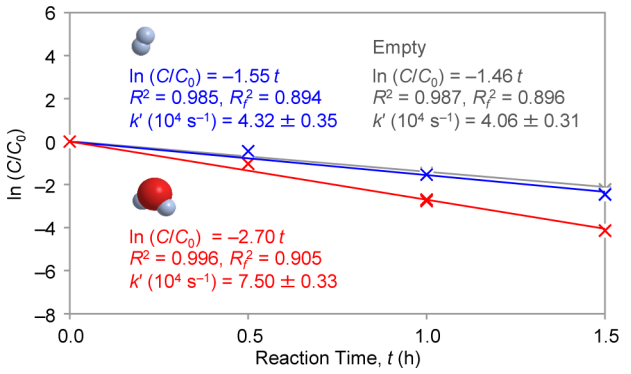

Figure 8. Plots of ln (C/C_0) versus reaction time, where C is the concentration of X@$C_{59}N$ dimers, C_0 the initial concentration of X@$C_{59}N$ dimers, t the reaction time, R^2 the coefficient of determination, R_f^2 the adjusted R^2, and k' the pseudo-first-order rate constant: red for $H_2O@C_{59}N$ dimers, blue for $H_2@C_{59}N$ dimers, and gray for $(C_{59}N)_2$.

dimers, 4.32 ± 0.35 for $H_2@C_{59}N$ dimers, and 4.06 ± 0.31 for $(C_{59}N)_2$. The rate constant k' for $H_2O@C_{59}N$ dimers was found to be absolutely larger than that for $(C_{59}N)_2$ (by 1.85 ± 0.16) even though there was little practical difference between $H_2@C_{59}N$ dimers and empty $(C_{59}N)_2$ ($k'(H_2)/k'$(empty) = 1.06 ± 0.12).

Theoretical Calculations. We estimated the stabilization energies for trapping H_2O inside the cage of C_{60}, MeC_{60}^-, MeC_{60}^+, $HC_{59}N$, $C_{59}N^-$, and $C_{59}N^+$ at the MP2/6-31G(d,p)//M06-2X/6-31G(d,p) level of theory with the basis set superposition error (BSSE) correction (Table S16 and Figure S32). For all species except for C_{60}, two conformers of a water molecule were found. Here, we focused on only the most stable conformers. For $H_2O@MeC_{60}^-$, the relative stabilization energy was calculated to be −7.3 kcal/mol, which was larger than that for C_{60} (−6.4 kcal/mol). The extra stabilization may come from the effect of hydrogen bonding between anionic center of MeC_{60}^- and H_2O as reported by Martín and co-workers.[34] For N-doped fullerene, $H_2O@HC_{59}N$ has the stabilization energy of −7.0 kcal/mol, which was almost the same value as $H_2O@MeC_{60}^-$ (isoelectronic carbon cage). Thus, it is no wonder that some kind of interaction exists in $H_2O@HC_{59}N$. This result supports the N−O interaction anticipated from relaxation time measurements and electrostatic potential maps. For $H_2O@C_{59}N^+$ with the largest stabilization energy (−8.8 kcal/mol), there should be a possible interaction between cationic center of $C_{59}N^+$ and entrapped H_2O (Figure 9). This may cause the

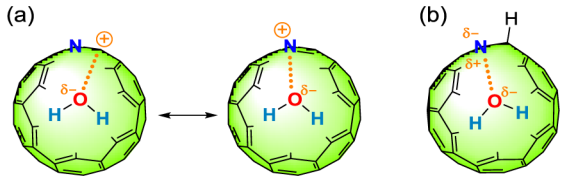

Figure 9. Most stable conformers suggested by DFT calculations (Table S16 and Figure S32): (a) $H_2O@C_{59}N^+$ having both carbenium and iminium cation characters and (b) an analogous structure of neutral $H_2O@HC_{59}N$. The caged bonds were partially omitted for clarity.

difference in reactivity upon the reaction of X@$C_{59}N$ dimers and acetone. In conclusion, the electrostatic interaction was suggested both in neutral state ($H_2O@HC_{59}N$) and in cationic state ($H_2O@C_{59}N^+$) from experimental and theoretical points of view.

SUMMARY

We developed methods for the synthesis of endohedral aza[60]fullerenes and obtained X@$C_{59}N$ (X = H_2O and H_2) as their dimers and monomers in several tens of milligrams quantities. We showed that *endohedral heterofullerenes* have unprecedented significance as a unique molecular system. The ^1H NMR spectrum of X@$C_{59}N$ dimers consisting of $(C_{59}N)_2$, X@$(C_{59}N)_2$, and $(X@C_{59}N)_2$ showed that there is no detectable magnetic interaction between two entrapped molecules separated by each cage and that the inner space of the $C_{59}N$ cage is more shielded than that of C_{60}. From the HPLC analyses, $(C_{59}N)_2$, $H_2O@(C_{59}N)_2$, and $(H_2O@C_{59}N)_2$ were found to be distinguishable from each other in contrast to $H_2@C_{59}N$ dimers. The T_1 measurements demonstrated that $H_2O@C_{59}N$ dimers have a 3-fold value compared to that of $H_2O@C_{60}$. We revealed the different relaxation mechanisms among X@C_{60} and X@$RC_{59}N$. The DFT calculations suggested a possibility of the attractive electrostatic interaction between a nitrogen atom on the $C_{59}N$ cage and entrapped H_2O and showed the rotational energy barrier of H_2O inside the $C_{59}N$ cage (1.46 kcal/mol). This might drastically impact the longer T_1 value for $H_2O@C_{59}N$ dimers. We were able to provide experimental evidence for the existence of positive potential which is located on the backside of the nitrogen atom. From the results of the competition experiment of X@$C_{59}N$ dimers and acetone under oxidative conditions, the difference in reactivity between $H_2O@C_{59}N$ and $H_2@C_{59}N$ dimers was observed ($k'(H_2O)/k'(H_2)$ = 1.74 ± 0.16). This result was in accordance with the prediction from the DFT calculations that $C_{59}N^+$ should be stabilized by entrapped H_2O via electrostatic interaction.

DOI: 10.1021/jacs.5b12795
J. Am. Chem. Soc. 2016, 138, 4096−4104

■ ASSOCIATED CONTENT

Supporting Information

The Supporting Information is available free of charge on the ACS Publications website at DOI: 10.1021/jacs.5b12795.

Supplementary figures and tables, detailed experimental procedures, characterization data, and computational results (PDF)

■ AUTHOR INFORMATION

Corresponding Author

*yasujiro@scl.kyoto-u.ac.jp

Notes

The authors declare no competing financial interest.

■ ACKNOWLEDGMENTS

Financial support was partially provided by the PRESTO program on "Molecular Technology and Creation of New Functions" from the JST, the JSPS KAKENHI (Grants 23241032 and 15K13641), and Grant-in-Aids for Scientific Research on Innovative Areas "π-System Figuration: Control of Electron and Structural Dynamism for Innovative Functions" and "Stimuli-responsive Chemical Species for the Creation of Functional Molecules" from the MEXT, Japan. We are grateful to Prof. Kenji Sugase at the Department of Molecular Engineering, Graduate School of Engineering, Kyoto University for fruitful discussion on NMR. This paper is dedicated to the memory of the late Prof. Nicholas J. Turro.

■ REFERENCES

(1) Saunders, M.; Jiménez-Vázquez, H. A.; Cross, R. J.; Poreda, R. J. *Science* **1993**, *259*, 1428−1430.

(2) Komatsu, K.; Murata, M.; Murata, Y. *Science* **2005**, *307*, 238−240.

(3) Kurotobi, K.; Murata, Y. *Science* **2011**, *333*, 613−616.

(4) Murphy, T. A.; Pawlik, T.; Weidinger, A.; Höhne, M.; Alcala, R.; Spaeth, J.-M. *Phys. Rev. Lett.* **1996**, *77*, 1075−1078.

(5) (a) Knapp, C.; Weiden, N.; Käss, H.; Dinse, K.-P.; Pietzak, B.; Waiblinger, M.; Weidinger, A. *Mol. Phys.* **1998**, *95*, 999−1004. (b) Weidinger, A.; Pietzak, B.; Waiblinger, M.; Lips, K.; Nuber, B.; Hirsch, A. *AIP. Conf. Proc.* **1998**, *442*, 363−367.

(6) Aoyagi, S.; Nishibori, E.; Sawa, H.; Sugimoto, K.; Takata, M.; Miyata, Y.; Kitaura, R.; Shinohara, H.; Okada, H.; Sakai, T.; Ono, Y.; Kawachi, K.; Yokoo, K.; Ono, S.; Omote, K.; Kasama, Y.; Ishikawa, S.; Komuro, T.; Tobita, H. *Nat. Chem.* **2010**, *2*, 678−683.

(7) Beduz, C.; Carravetta, M.; Chen, J. Y.-C.; Concistrè, M.; Denning, M.; Frunzi, M.; Horsewill, A. J.; Johannessen, O. G.; Lawler, R.; Lei, X.; Levitt, M. H.; Li, Y.; Mamone, S.; Murata, Y.; Nagel, U.; Nishida, T.; Ollivier, J.; Rols, S.; Rõõm, T.; Sarkar, R.; Turro, N. J.; Yang, Y. *Proc. Natl. Acad. Sci. U. S. A.* **2012**, *109*, 12894−12898.

(8) Aoyagi, S.; Hoshino, N.; Akutagawa, T.; Sado, Y.; Kitaura, R.; Shinohara, H.; Sugimoto, K.; Zhang, R.; Murata, Y. *Chem. Commun.* **2014**, *50*, 524−526.

(9) (a) Guo, T.; Jin, C.; Smalley, R. E. *J. Phys. Chem.* **1991**, *95*, 4948. (b) Dunk, P. W.; Rodríguez-Fortea, A.; Kaiser, N. K.; Shinohara, H.; Poblet, J. M.; Kroto, H. W. *Angew. Chem., Int. Ed.* **2013**, *52*, 315.

(10) Pradeep, T.; Vijayakrishnan, V.; Santra, A. K.; Rao, C. N. R. *J. Phys. Chem.* **1991**, *95*, 10564.

(11) Kimura, T.; Sugai, T.; Shinohara, H. *Chem. Phys. Lett.* **1996**, *256*, 269.

(12) Poblet, J. M.; Muñoz, J.; Winkler, K.; Cancilla, M.; Hayashi, A.; Lebrilla, C. B.; Balch, A. L. *Chem. Commun.* **1999**, 493.

(13) Hummelen, J. C.; Prato, M.; Wudl, F. *J. Am. Chem. Soc.* **1995**, *117*, 7003−7004.

(14) Hummelen, J. C.; Knight, B.; Pavlovich, J.; González, R.; Wudl, F. *Science* **1995**, *269*, 1554−1556.

(15) Keshavarz-K, M.; González, R.; Hicks, R. G.; Srdanov, G.; Srdanov, V. I.; Collins, T. G.; Hummelen, J. C.; Bellavia-Lund, C.; Pavlovich, J.; Wudl, F.; Holczer, K. *Nature* **1996**, *383*, 147−150.

(16) Nuber, B.; Hirsch, A. *Chem. Commun.* **1996**, 1421−1422.

(17) Chai, Y.; Guo, T.; Jin, C.; Haufler, R. E.; Chibante, L. P. F.; Fure, J.; Wang, L.; Alford, J. M.; Smalley, R. E. *J. Phys. Chem.* **1991**, *95*, 7564−7568.

(18) Akasaka, T.; Okubo, S.; Wakahara, T.; Yamamoto, K.; Kobayashi, K.; Nagase, S.; Kato, T.; Kako, M.; Nakadaira, Y.; Kitayama, Y.; Matsuura, K. *Chem. Lett.* **1999**, 945−946.

(19) Zuo, T.; Xu, L.; Beavers, C. M.; Olmstead, M. M.; Fu, W.; Crawford, T. D.; Balch, A. L.; Dorn, H. C. *J. Am. Chem. Soc.* **2008**, *130*, 12992−12997.

(20) Fu, W.; Zhang, J.; Fuhrer, T.; Champion, H.; Furukawa, K.; Kato, T.; Mahaney, J. E.; Burke, B. G.; Williams, K. A.; Walker, K.; Dixon, C.; Ge, J.; Shu, C.; Harich, K.; Dorn, H. C. *J. Am. Chem. Soc.* **2011**, *133*, 9741−9750.

(21) Stevenson, S.; Ling, Y.; Coumbe, C. E.; Mackey, M. A.; Confait, B. S.; Phillips, J. P.; Dorn, H. C.; Zhang, Y. *J. Am. Chem. Soc.* **2009**, *131*, 17780−17782.

(22) Stevenson, S.; Thompson, M. C.; Coumbe, H. L.; Mackey, M. A.; Coumbe, C. E.; Phillips, J. P. *J. Am. Chem. Soc.* **2007**, *129*, 16257−16262.

(23) (a) Rubin, Y. *Chem. - Eur. J.* **1997**, *3*, 1009−1016. (b) Murata, M.; Murata, Y.; Komatsu, K. *Chem. Commun.* **2008**, 6083−6094. (c) Komatsu, K.; Murata, Y. *Chem. Lett.* **2005**, *34*, 886−891.

(24) Krachmalnicoff, A.; Levitt, M. H.; Whitby, R. J. *Chem. Commun.* **2014**, *50*, 13037−13040.

(25) (a) Prato, M.; Li, Q. C.; Wudl, F. *J. Am. Chem. Soc.* **1993**, *115*, 1148−1150. (b) Grösser, T.; Prato, M.; Lucchini, V.; Hirsch, A.; Wudl, F. *Angew. Chem., Int. Ed. Engl.* **1995**, *34*, 1343−1345.

(26) Hashikawa, Y.; Murata, M.; Wakamiya, A.; Murata, Y. *Org. Lett.* **2014**, *16*, 2970−2973.

(27) Zhang, R.; Murata, M.; Wakamiya, A.; Murata, Y. *Chem. Lett.* **2013**, *42*, 879−881.

(28) Frisch, M. J.; Trucks, G. W.; Schlegel, H. B.; Scuseria, G. E.; Robb, M. A.; Cheeseman, J. R.; Scalmani, G.; Barone, V.; Mennucci, B.; Petersson, G. A.; Nakatsuji, H.; Caricato, M.; Li, X.; Hratchian, H. P.; Izmaylov, A. F.; Bloino, J.; Zheng, G.; Sonnenberg, J. L.; Hada, M.; Ehara, M.; Toyota, K.; Fukuda, R.; Hasegawa, J.; Ishida, M.; Nakajima, T.; Honda, Y.; Kitao, O.; Nakai, H.; Vreven, T.; Montgomery, Jr., J. A.; Peralta, J. E.; Ogliaro, F.; Bearpark, M.; Heyd, J. J.; Brothers, E.; Kudin, K. N.; Staroverov, V. N.; Keith, T.; Kobayashi, R.; Normand, J.; Raghavachari, K.; Rendell, A.; Burant, J. C.; Iyengar, S. S.; Tomasi, J.; Cossi, M.; Rega, N.; Millam, J. M.; Klene, M.; Knox, J. E.; Cross, J. B.; Bakken, V.; Adamo, C.; Jaramillo, J.; Gomperts, R.; Stratmann, R. E.; Yazyev, O.; Austin, A. J.; Cammi, R.; Pomelli, C.; Ochterski, J. W.; Martin, R. L.; Morokuma, K.; Zakrzewski, V. G.; Voth, G. A.; Salvador, P.; Dannenberg, J. J.; Dapprich, S.; Daniels, A. D.; Farkas, O.; Foresman, J. B.; Ortiz, J. V.; Cioslowski, J.; Fox, D. J. *Gaussian 09*, revision B.01; Gaussian Inc.: Wallingford, CT, 2010.

(29) (a) Cross, B. P.; Schleich, T. *Org. Magn. Reson.* **1977**, *10*, 82−85. (b) Jameson, C. J. *Annu. Rev. Phys. Chem.* **1996**, *47*, 135−169. (c) Stringfellow, T. C.; Farrar, T. C. *Spectrochim. Acta, Part A* **1997**, *53*, 2425−2433.

(30) (a) Sartori, E.; Ruzzi, M.; Turro, N. J.; Decatur, J. D.; Doetschman, D. C.; Lawler, R. G.; Buchachenko, A. L.; Murata, Y.; Komatsu, K. *J. Am. Chem. Soc.* **2006**, *128*, 14752−14753. (b) Li, Y.; Chen, J. Y.-C.; Lei, X.; Lawler, R. G.; Murata, Y.; Komatsu, K.; Turro, N. J. *J. Phys. Chem. Lett.* **2012**, *3*, 1165−1168.

(31) (a) Rubin, Y.; Jarrosson, T.; Wang, G.-W.; Bartberger, M. D.; Houk, K. N.; Schick, G.; Saunders, M.; Cross, R. J. *Angew. Chem., Int. Ed.* **2001**, *40*, 1543−1546. (b) Chen, J. Y.-C.; Martí, A. A.; Turro, N. J.; Komatsu, K.; Murata, Y.; Lawler, R. G. *J. Phys. Chem. B* **2010**, *114*, 14689−14695.

(32) (a) Ito, S.; Tokimaru, Y.; Nozaki, K. *Angew. Chem., Int. Ed.* **2015**, *54*, 7256−7260. (b) Yokoi, H.; Hiraoka, Y.; Hiroto, S.; Sakamaki, D.; Seki, S.; Shinokubo, H. *Nat. Commun.* **2015**, *6*, 8215.

DOI: 10.1021/jacs.5b12795
J. Am. Chem. Soc. 2016, 138, 4096−4104

(33) (a) Hauke, F.; Hirsch, A. *Chem. Commun.* **1999**, 2199−2200. (b) Hauke, F.; Hirsch, A. *Tetrahedron* **2001**, *57*, 3697−3708.
(34) Maroto, E. E.; Mateos, J.; Garcia-Borràs, M.; Osuna, S.; Filippone, S.; Herranz, M. Á.; Murata, Y.; Solà, M.; Martín, N. *J. Am. Chem. Soc.* **2015**, *137*, 1190−1197.

DOI: 10.1021/jacs.5b12795
J. Am. Chem. Soc. 2016, 138, 4096−4104